AIAA JOURNAL
Vol. 50, No. 12, December 2012

Automated, Real-Time Health Monitoring of Structures for Interplanetary Exploration Systems

Shannon M. Statham* and Sathya V. Hanagud†
Georgia Institute of Technology, Atlanta, Georgia 30332
and
Brian J. Glass‡
NASA-Ames Research Center, Moffett Field, California 94035

DOI: 10.2514/1.J051173

Space exploration missions, specifically to Mars, involve complex operations as the search for water and other signs of extant or past life continues. Such missions require advanced robotic systems that are susceptible to structural and mechanical failures and operational faults, which motivates a need for structural health monitoring techniques relevant to interplanetary exploration systems. This paper presents an automated dynamics-based structural health monitoring system using laser Doppler velocimeter sensors, signal filters, and trained neural networks that is formulated for a subsurface interplanetary exploration drill prototype. The developed system presents advanced research accomplishments in the area of real-time structural health monitoring that include rapid-response capabilities of predicting drilling faults and failures before they occur and field demonstrations on an operating drill system.

Nomenclature

B_i	=	constants of spatial solution, $i = 1, 2, \ldots, m$
b_f	=	length of drill auger tube flanges (cross section), in.
D	=	nondimensional spring constant for drilling model translational elastic foundation
d_i	=	inner diameter of drill auger tube, in.
d_o	=	outer diameter of drill auger tube, in.
E	=	modulus of elasticity, Pa
f_n	=	nth harmonic frequency of gearbox system, Hz
f_r	=	gear rotation speed, Hz
$H(z)$	=	frequency domain function of Chebyshev type I filter
h_f	=	height of drill auger tube flanges (cross section), in.
I	=	cross-sectional area moment of inertia, m^4
L	=	length of drill auger tube, m
L'	=	position of jamming fault along z-axis, m
m	=	mass per unit length, lb/m
P	=	compressive tip load, N
Q	=	number of teeth in gearbox system
S_B	=	nondimensional rotational spring constant for drill supports
S_K	=	nondimensional translational spring constant for drill supports
t	=	time, s
U	=	spatial solution for lateral deflection, m
U_L, U_R	=	lateral spatial deflections along a split axis (left, right), m
$u_i(z, t)$	=	deflections of elastic beam, $i = 1, 2, 3$ for (x, y, z) axes, m
$w(t)$	=	noise in gear meshing vibration signal
(x, y, z)	=	local coordinate system
α	=	eigenvalues of spatial solution (lateral deflection)
β_S	=	rotational spring constant for drill supports, Nm/rad
β_Z	=	rotational spring constant for jamming fault model, Nm/rad
γ	=	equation of motion roots for nominal drilling model
δ	=	nondimensional position of drilling model elastic foundation along z-axis
η	=	nondimensional variable for position along z-axis
Θ	=	flute twist of helical drill auger tube, rpm
κ_D	=	spring constant for drilling model translational elastic foundation, N/m^2
κ_S	=	translational spring constant for drill supports, N/m
κ_Z	=	translational spring constant for jamming fault model, N/m
Ξ_n	=	amplitude of nth harmonic of gear meshing vibration
$\xi(t)$	=	gear meshing vibration
$\upsilon(t)$	=	axial velocity, m/s
Φ_n	=	phase angle of nth harmonic of gear meshing vibration, rad
$\Omega(t)$	=	angular velocity, rad/s
ω	=	frequency (natural frequencies, mesh frequencies, etc.), rad/s

Received 14 April 2011; revision received 15 December 2011; accepted for publication 5 April 2012.

*Ph.D. Candidate, School of Aerospace Engineering, 270 Ferst Drive NW. Member AIAA.
†Professor, 270 Ferst Drive NW. Fellow AIAA.
‡Senior Scientist, Exploration Systems Division, Mail Stop 269-4. Associate Fellow AIAA.

I. Introduction

STRUCTURAL health monitoring (SHM) is a process of detecting damages or other defects in structural and mechanical systems that adversely affect the current or future performance of these systems [1]. The principle behind many SHM techniques is that modal parameters (frequencies, mode shapes, curvature, etc.) are functions of the physical properties (mass, stiffness, damping, etc.) and boundary conditions of a structure. Therefore, any changes in the physical properties or boundary conditions of the system due to damage or other defects will alter the dynamic characteristics and modal parameters [2].

Modal parameters are easily identified from measured dynamic responses [3]. Dynamic responses are acquired by exciting the system with either external transducers (such as a piezoelectric actuator, shaker, or impact/impulse hammer) or ambient forces in the service environment and capturing the resulting dynamic response with sensors (such as strain gauges, accelerometers and laser Doppler velocimeters) [4–6].

In dynamics-based SHM techniques, the most common modal parameters used are natural frequencies, mode shapes, and mode shape curvatures. The most popular of the three are natural frequencies because they are easy to identify and require few sensors

[3,7–11]. Many studies, however, have found that natural frequencies are not sensitive enough to indicate the presence or location of damage unless very precise measurements have been obtained or large levels of damage have occurred [12]. A counterargument is that frequencies, specifically lower frequencies, are most affected by changes in boundary conditions due to damage or operating faults [13]. This concept is the premise of the presented SHM technique.

To search for evidence of extant or past microbial life and sources of water, and determine the geological makeup of Mars, acquisition of geological samples is necessary from subsurface depths estimated at tens to hundreds and thousands of meters [14,15]. Direct subsurface sampling is the most fundamental technique for exploring unaltered in-situ characteristics of any planetary subsurface, and drilling is necessary for subsurface exploration below a few centimeters [16,17]. Other options, such as mechanical excavation (scooping/scraping), explosives, and penetrators, have limitations with achievable depths, sample retrieval, and preservation of the subsurface region [18].

Near-term, in-situ resource utilization is to be accomplished with low-power, lightweight, rover-deployable or standalone drills capable of penetration a few tens of meters in depth. These drills need to include autonomous sample handling, down-hole scientific instruments, and drill diagnostics [16]. Two sister projects have completed the first stage of developing a suitable prototype for near-term space drilling missions: the Mars Astrobiology Research and Technology Experiment (MARTE) and the Drilling Automation for Mars Exploration (DAME). MARTE has demonstrated automated core handling and auger tube change outs, and field tested the developed hardware and software at a Mars-analog site in Rio Tinto, Spain [19,20]. DAME has demonstrated "smart" drilling [15,21] where the drill system autonomously executed a drilling plan and, equipped with on-board diagnostic modules, identified and recovered from expected drilling faults. DAME has field tested the developed hardware and software at a Mars-analog site on Devon Island, Canada. The bulk of the research work presented in this paper has been applied and field tested for the DAME drill system.

The following sections include detailed descriptions of the requirements, objectives, development, and procedure of the presented SHM technique. Field test results, validation, and directions for future research are also discussed.

II. Structural Health Monitoring Requirements and Objectives

The purpose of this research is to formulate and field test a dynamics-based SHM system for a drill prototype that is compatible with interplanetary subsurface exploration. Interplanetary exploration missions have strict and unique restrictions for an on-board SHM system that are different from most SHM techniques developed to date. These restrictions include the following:

1) The SHM system must monitor the drill system while it is in operation. Stopping or halting the drilling operation for SHM procedures such as dynamic response measurements is problematic, if not catastrophic, because of the extreme subsurface environment and time restrictions.

2) The SHM system must have autonomous, real-time capabilities. Complications involved with drilling unknown subsurface territories occur quickly and, because of communication delays with Earth, Earth-based direction of the drilling operation and SHM system is not practical. Thus, an autonomous and rapid-response SHM system is required.

3) The entire drilling operation is limited to the obtainable power on Mars. The available power is limited to the energy obtained from solar cells aboard the Mars interplanetary exploration system, which has been estimated to be 100 W for the DAME drill. This limitation on power also restricts the drilling performance parameters (rotation speed, rate of penetration, etc.), which further emphasizes the need for on-board diagnostic modules as drilling faults are more likely to occur with significantly restricted drilling parameters.

From these conditions, the formulated design requirements for an on-board SHM technique are as follows [22]:

1) The sensors, transducers, and analysis equipment should not interfere with the normal drilling operation.

2) Expected drilling fault conditions must be identified before the actual failure occurs (as a probability measure) to initiate appropriate corrective actions and allow for a continuous drilling operation.

3) The SHM technique must produce real-time diagnostics and have complete autonomous operations.

These unique and strict design requirements create a need for new and innovative methods to monitor the structural health of a dynamic system. More commonly practiced SHM techniques involve time-intensive inspections in depot environments and laboratories, and few studies have validated SHM methods for structural and mechanical systems while the structures are in use in their operating environment [1,12,13,23]. Therefore, to design and develop a real-time, automated SHM technique for an operating drill system, the following objectives were established:

1) Understand the base dynamic characteristics of the drill system.

2) Identify expected drilling faults based on experience and preliminary field tests.

3) Complete dynamic response and analysis experiments on the drill structure and determine the most efficient instruments, sensor equipment, and analysis tools for drilling applications.

4) Formulate structural dynamic models, with and without fault conditions, for the drill structure.

5) Automate a signal analysis procedure and produce diagnostics based on signal analysis and theoretical models.

6) Develop an automation procedure for the entire SHM system.

Additional design restrictions will need to be considered to implement the formulated SHM system for interplanetary exploration missions, such as size and weight limitations and the extreme operating environment. For example, further research and development for nontraditional sensors (e.g., laser Doppler velocimeters) is necessary to ensure compatibility with such missions. This discussion is beyond the scope of the presented paper, but comments and recommendations are provided in the Conclusions section.

III. Development and Procedure of Structural Health Monitoring

A. Preliminary Field Tests

The drill system of primary interest in this research was developed for NASA's collaborative DAME project. Two preliminary field tests on this drill system were conducted at the Haughton Crater Research Station (HCRS), which is a research station adjacent to the Haughton Crater on Devon Island, Canada. The Haughton Crater is located at $75^{o}22'$ N latitude and $89^{o}41'$ W longitude, and it is a prime location for testing Mars drills because it has subsurface ice and permafrost that are expected in higher Martian latitudes [15,24,25].

The goals of these preliminary field tests were to test the drill hardware, identify the most common and expected drilling faults, and construct a procedure for the drilling operations and automation software. Drilling faults are defined as any condition that hinders progress with the normal drilling procedure and, if not dealt with in a timely manner, has the potential to cause a catastrophic event for the drill structure and mission. Six unique drilling faults were identified and classified during the preliminary field tests: binding, choking, bit inclusion, jamming, hard material, and corkscrewing [26]. Sketches of the drilling faults are provided in Fig. 1, and the classification of each fault was as follows:

1) Binding: a rock protrudes from the bore-hole wall, causing the auger to catch on the rock each time it rotates. This fault is most commonly associated with increasing or spiking torque on the auger tube.

2) Choking: the cuttings build up in the auger flutes, causing an increase in pressure between the bore-hole wall and auger tube. This fault is most commonly associated with a gradual increase in torque on the auger tube and fluctuating rate of penetration.

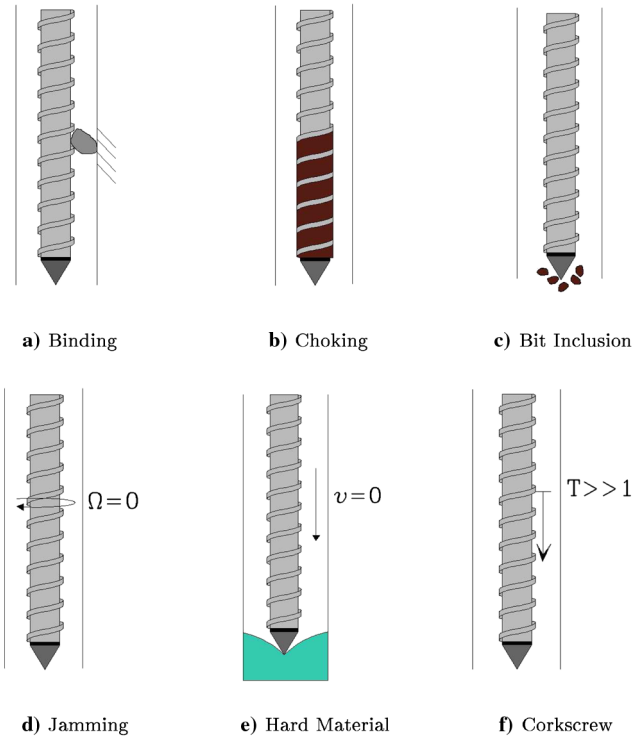

Fig. 1 Sketches of identified drilling faults.

3) Bit inclusion: the bit catches on a pebble or rock at the bottom of the hole. This fault is most commonly associated with torque spikes at the bit.

4) Jamming: an extreme condition of binding, choking, and/or bit inclusion where the auger tube completely stops rotating. This fault is most commonly associated with a sudden decrease or halt in the rotational speed of the drill.

5) Hard material: the drill encounters a hard formation in the ground and cannot proceed with the normal cutting bit. This fault is most commonly associated with a decreasing rate of penetration.

6) Corkscrewing: the auger flutes rub against the bore-hole wall and apply reverse screw tension from the ground. This fault is most commonly associated with large tensile forces on the auger tube.

Other findings during the preliminary field tests were dynamic characteristics unique to the drilling system, which helped formulate the structural dynamic models of the drill. These findings included the following:

1) The dynamic response of the drill auger tube is sufficient for determining the dynamic characteristics of the drill structure and analyzing the drill condition.

2) Under nominal drilling conditions, given the restricted power consumption, the rotational speed, rate of penetration, and down-hole force have negligible effects on the dynamic response of the drill auger tube.

3) The vibrations created by the drilling operation adequately excite the dynamic response of the drill auger tube for dynamic measurements.

4) The drill's gearbox system produces incremental frequencies in the signal response of the drill that can interfere with the signal analysis and diagnostics.

B. Modal Analysis Experiments

To understand the dynamic characteristics of the drill system and determine the most efficient sensor equipment for this application, modal analysis experiments have been conducted on the drill system. The natural frequencies of the auger tube were obtained using an impulse hammer and two sensor types, accelerometer and laser Doppler velocimeter (LDV), while the drill system was stationary. A SigLab data acquisition (DAQ) system [27] was used to record the signal from the sensors and impulse hammer and provide the dynamic response of the auger tube. Figure 2 provides a diagram of the experimental setup.

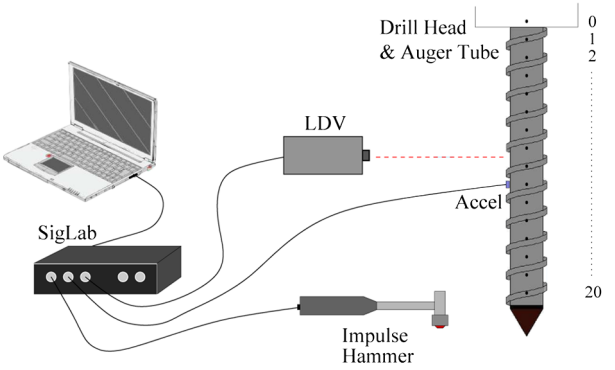

Fig. 2 Diagram of equipment setup for modal analysis experiments.

Laser Doppler velocimetry is a technique for measuring the dynamic response of a moving object by measuring the component of velocity along the laser line of sight [28]. LDV sensors have significant advantages in the SHM field and unique capabilities compared with the more commonly used contact sensors (accelerometers, strain gauges, etc.) [29,30]. LDV sensors are optical sensors that do not require contact with the system being measured. This allows much flexibility in the sensor positioning and isolates the sensor from the drill auger tube. Contact-based sensors also require use of the limited bus lines available inside the auger tube and create mass-loading effects, which makes the dynamic measurements more difficult to compare with theoretical models. LDV sensors do not suffer from these constraints. Therefore, another important aspect of these modal analysis experiments was to validate the use of LDV sensors.

Figure 3 provides the magnitude of a sample frequency response function (FRF) of the stationary auger tube using an impulse hammer for dynamic excitation. The plot shows the response captured by the accelerometer and LDV sensor and the first two natural frequencies of the stationary auger tube (peaks indicated with asterisks). The plot also demonstrates great correlation between the measured response of the two sensors, which validates the accuracy of LDV sensors for this application.

For simplification, the damping coefficient of the auger tube is assumed small, and the natural frequencies are therefore selected as the peaks in the dynamic response [9]. From these experiments, the first two natural frequencies of the stationary auger tube were found to be 9 and 95 Hz.

Modal analysis experiments while the auger tube was rotating in place were conducted to confirm that the drill motor system adequately excited the drill system and nominal rotational speed conditions had negligible effects on the dynamic response of the auger tube. The dynamic response of the drill rotating at 10 and

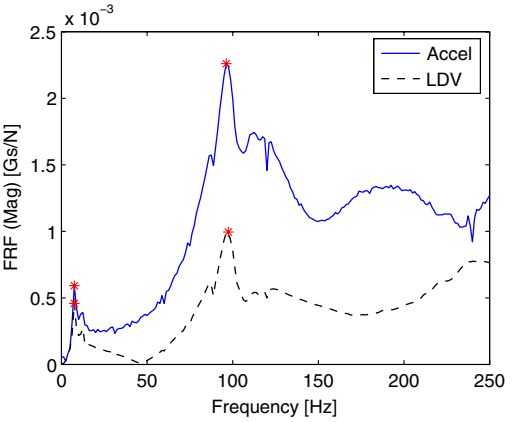

Fig. 3 Impulse hammer dynamic response of stationary drill auger tube.

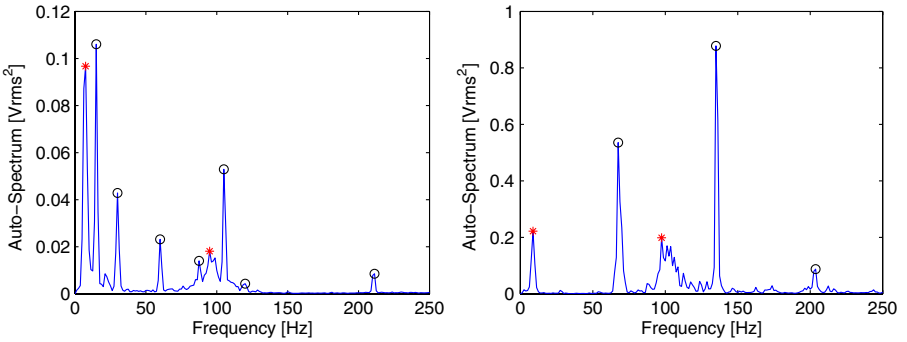

a) 10 RPM **b) 45 RPM**

Fig. 4 Rotating dynamic response of drill auger tube.

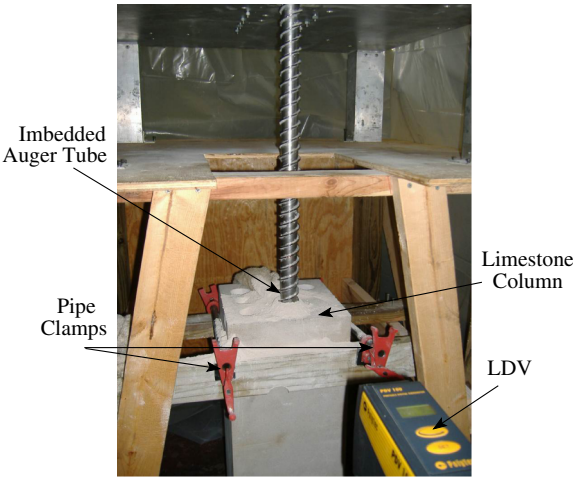

Fig. 5 Drill system setup for drilling experiments.

45 rpm is provided in Fig. 4, and the first two natural frequencies of the auger tube are indicated by asterisks. It is also important to note the incremental frequencies present in these frequency responses (peaks indicated by circles). These frequencies are created by the drill's gearbox system and are present whenever the drill motors are in operation.

Other modal analysis experiments conducted on the drill system included drilling tests and multidimensional measurement tests. Drilling tests involved drilling into a fixed limestone column ($28 \times 28 \times 91$ cm) up to a 70-cm depth ($\approx$2.3 ft). Limestone was chosen for these experiments because it is a softer sedimentary rock that can test the drill system under nominal drilling conditions expected in the field. Figure 5 provides a photograph of the experimental setup, and Table 1 provides the first two natural frequencies of the auger tube identified for various drill depths.

Finally, multidimensional measurement tests were conducted to analyze the response of the auger tube from different positions of the LDV sensor. Figure 6 provides the magnitude of the frequency response function for the same location on the auger tube from two orthogonal positions. Although similar, there are distinct differences between the two lateral frequencies, which showed a dependence of the dynamic response on the position of the LDV sensors. These results motivated a multidimensional analysis of the drill system using multiple LDV sensors [31]. Because the cost and number of sensors are important factors, specifically for interplanetary exploration missions, capturing the dynamic response of the drill in multiple dimensions using one LDV sensor is also valuable and is currently being investigated.

Table 1 Auger tube natural frequencies

Auger length, m	Drill depth, cm	Embedded auger, %	1st mode, Hz	2nd mode, Hz
1	0	0	9	95
1	10	10	41	111
1	20	20	58	119
1	30	30	71	131
2	30	15	17	60
2	40	20	20	61
2	50	25	23	62
2	60	30	36	81
2	70	35	42	94

C. Structural Dynamic Models

Developing models, with and without damage or defects, is essential in the SHM field to understand, analyze, and interpret the health of structural dynamics systems. Model development provides a theoretical basis that allows engineers to predict the behavior of structures under various circumstances and damage.

The drill auger tube is visualized as a moving and rotating fixed-free beam supported by the drill head and platform. The auger tube is a hollow, stainless steel tube with helical flutes that wind along the length of the auger and enable the removal of cuttings to the surface during the drilling process. In operation, the auger tube has a compressive tip load because of the applied down-hole force, and the total length changes with time as the depth increases and more auger tube strings are added. A photograph and sketch of the subsurface exploration drill investigated in this research is shown in Fig. 7.

Assuming the two orthogonal lateral motions are decoupled from torsional and axial motions, a two-dimensional continuum model was developed. The drill auger tube is thus modeled as a fixed-free beam with length $L(t)$, axial velocity $\upsilon(t)$, angular velocity $\Omega(t)$, compressive tip load P, flute twist Θ, and lateral displacements $u_1(z, t)$ and $u_2(z, t)$ in the x and y directions, respectively (Fig. 8).

The most critical aspect of the developed SHM technique is accurate, reliable, and rapid real-time diagnosis of the drilling condition. Therefore, simple and reliable dynamic models are more efficient than complex models or techniques (such as wave-based SHM techniques) for this specific application. From the preliminary field tests, modal analysis experiments, and analysis of the initial auger tube model (Fig. 8) using Galerkin's method and finite element analysis [32], it was determined that the angular velocity, axial velocity, and compressive tip load (under nominal drilling conditions) have negligible effects on the dynamic characteristics of the auger tube and therefore are neglected. As the auger tube strings are added and removed when needed, the length of the current auger tube is fixed for a set amount of time t. To simplify the complex geometry because of the auger flutes, it was also determined (through finite element analysis) that a constant cross section could be used assuming a constant cross-sectional area moment of inertia about the x axis: $I = I_{xx}$ [32]. Finally, when comparing the modal analysis experiments with the fixed-free beam model, it was determined that a fixed connection between the auger tube and drill head does not accurately represent the drill system. Therefore, the fixed end was replaced with spring constraints. The modified one-dimensional

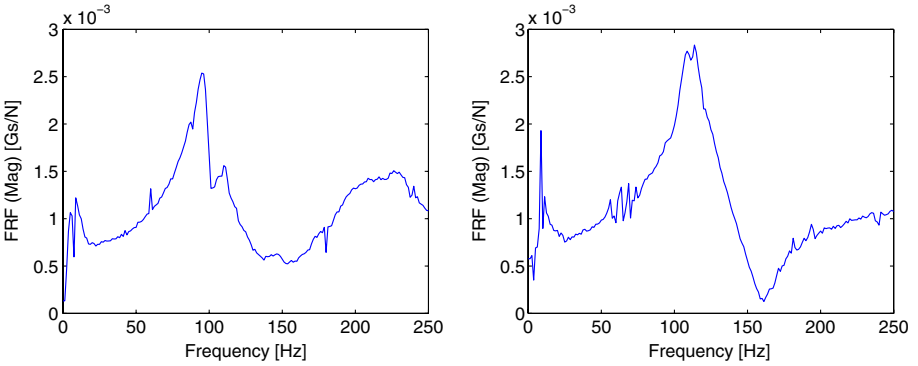

a) Front **b) Side**

Fig. 6 Impulse hammer dynamic response of same position on auger tube from two orthogonal directions.

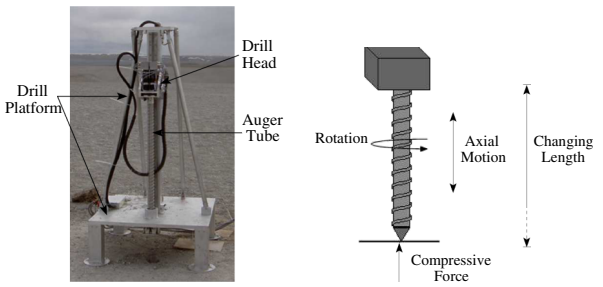

Fig. 7 Photograph and sketch of DAME drill.

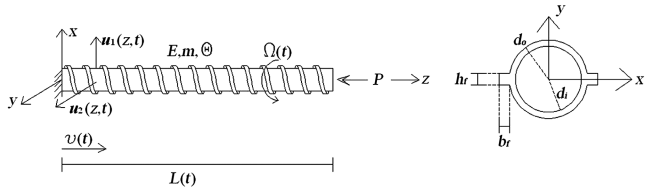

Fig. 8 Original model for drill auger tube.

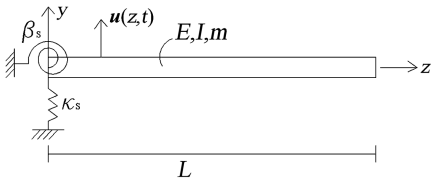

Fig. 9 Simplified base model of drill auger tube.

model is provided in Fig. 9, and the material and geometric properties are provided in Table 2.

Using Euler–Bernoulli beam theory, the equation of motion for $u(z, t)$ and the boundary conditions for the drill model are

$$EI\frac{\partial^4 u(z,t)}{\partial z^4} + m\frac{\partial^2 u(z,t)}{\partial t^2} = 0, \qquad 0 < z < L \tag{1}$$

$$z = 0\text{: } EI\frac{d^3u(z)}{dz^3} + \kappa_s u(z) = 0, \qquad EI\frac{d^2u(z)}{dz^2} - \beta_s\frac{du(z)}{dz} = 0,$$
$$z = L\text{: } EI\frac{d^3u(z)}{dz^3} = 0, \qquad EI\frac{d^2u(z)}{dz^2} = 0 \tag{2}$$

Assuming simple harmonic motions and applying separation of variables, the solution for Eq. (1) has the form

$$u(z, t) = U(z)e^{i\omega t} \tag{3}$$

and the spatial solution, nondimensionalized by the length of the beam (L), is

$$U(\eta) = B_1\cosh(\alpha\eta) + B_2\sinh(\alpha\eta) + B_3\cos(\alpha\eta) + B_4\sin(\alpha\eta) \tag{4}$$

where $\eta = z/L$ and $\alpha^4 = \omega^2(mL^4/EI)$.

Substituting Eq. (4) in the boundary conditions, the characteristic equation for the drill model was found [Eq. (5)]. The values for κ_s and β_s are evaluated by substituting the first two natural frequencies found from the modal analysis experiments of the stationary auger tube for ω_n (9 and 95 Hz). The values for κ_s and β_s were found to be 712 kN/m and 4706 Nm/rad, respectively.

$$\alpha^4 - (\alpha^4 - S_K S_B)\cosh(\alpha)\cos(\alpha) + (\alpha S_K - \alpha^3 S_B)\sinh(\alpha)\cos(\alpha)$$
$$- (\alpha S_K + \alpha^3 S_B)\cosh(\alpha)\sin(\alpha) + S_K S_B = 0$$
$$S_K = \frac{\kappa_s L^3}{EI}, \qquad S_B = \frac{\beta_s L}{EI}, \qquad \alpha^4 = \alpha_n^4 = \omega_n^2\frac{mL^4}{EI},$$
$$n = 1, 2, 3, \ldots \tag{5}$$

Next, a model for the nominal drilling condition is needed. Many drilling studies either use clamped or pinned conditions for the end/embedded boundary condition [33,34]. However, as evident from the results in Table 1, the natural frequencies of the auger tube increase with increasing depth, and a constant boundary condition to represent the embedded drilling auger is not appropriate for this application. Therefore, a moving Winkler-type elastic foundation is used to model the embedded drilling auger [35]. The developed drilling model is illustrated in Fig. 10, and the equations of motion are

$$EI\frac{\partial^4 u}{\partial z^4} + m\frac{\partial^2 u}{\partial t^2} = 0, \qquad 0 < z < L\text{-depth} \tag{6}$$

$$EI\frac{\partial^4 u}{\partial z^4} + m\frac{\partial^2 u}{\partial t^2} + \kappa_D u = 0, \qquad L\text{-depth} \le z < L \tag{7}$$

Using separation of variables and nondimensionalizing by the length of the beam (L), the spatial solution is

Table 2 Geometric and material properties of drill auger tube

Property	Symbol	Value	Units
Inner diameter	d_i	3.175	cm
Outer diameter	d_o	3.708	cm
Length of flanges	b_f	0.508	cm
Height of flanges	h_f	0.762	cm
Length	L	100	cm
Mass per unit length	m	3.856	kg/m
Modulus of elasticity	E	197e9	Pa

$$0 < \eta < \delta\text{: } U_L(\eta) = B_1\cosh(\alpha\eta) + B_2\sinh(\alpha\eta) + B_3\cos(\alpha\eta) + B_4\sin(\alpha\eta),$$

$$\delta \le \eta < 1\text{: } U_R(\eta) = \begin{cases} B_5\cosh(\gamma\eta) + B_6\sinh(\gamma\eta) + B_7\cos(\gamma\eta) + B_8\sin(\gamma\eta), & \alpha^4 \ge D \\ [B_5\cosh(\gamma\eta)\cos(\gamma\eta) + B_6\sinh(\gamma\eta)\cos(\gamma\eta) + B_7\cosh(\gamma\eta)\sin(\gamma\eta) + B_8\sinh(\gamma\eta)\sin(\gamma\eta)], & \alpha^4 < D \end{cases} \tag{8}$$

where

$$\delta = 1 - \frac{\text{depth}}{L}, \qquad D = \frac{\kappa_D L^4}{EI}$$

$$\gamma = \begin{cases} (\alpha^4 - D)^{1/4}, & \alpha^4 > D \\ ((D - \alpha^4)/4)^{1/4}, & \alpha^4 < D \end{cases}$$

The boundary conditions are the same as the simplified base model [Eq. (2)], and, for continuity, the following must be true at $\eta = \delta$:

$$\frac{d^i U_L}{d\eta^i} = \frac{d^i U_R}{d\eta^i}, \qquad i = 1, 2, 3 \tag{9}$$

Substituting Eq. (8) in the boundary conditions [Eq. (2)] and continuity equations [Eq. (9)], the characteristic equation and natural frequencies are evaluated. The changes in natural frequencies of a 1-m auger tube for various drill depths and values of κ_D are illustrated in Fig. 11. These results show a significant but gradual change in the auger tube frequencies as a function of drill depth using the formulated nominal drilling model. These results also demonstrate a better correlation with the experimental results (Table 1) compared with the clamped or pinned boundary condition for the embedded auger tube.

Similar to the evaluation of κ_s and β_s for the base drill model, the value for κ_D is calculated using the natural frequencies and drill depths from the nominal drilling experiments (Table 1) and the derived characteristic equation of the nominal drilling model. From this analysis, the mean value of κ_D was found to be 1333 kN/m^2.

To model the six drilling faults, it is assumed that each fault condition uniquely alters the dynamic characteristics of the drill system, specifically the boundary conditions. As the lower frequencies are most sensitive to changes in boundary conditions, the natural frequencies of the drill system are used to predict any changes in the boundary conditions and, thus, the condition of the drilling operation. Therefore, each drilling fault is carefully analyzed to determine what dynamic changes are expected and how to appropriately model these changes.

An example of a drilling fault model (jamming) is provided in Fig. 12. Jamming is visualized as a restriction to all motion at the location of the jam and is modeled with spring supports (κ_z and β_z) at location L'.

Similar to the nominal drilling model, the characteristic equation for the jamming fault model is derived using the spatial solution, boundary conditions, and continuity conditions, and the natural frequencies are evaluated for specified values of L', κ_z, and β_z. The location of the jam (L') can exist anywhere along the embedded auger (L-depth $\le L' \le L$), and the values of κ_z and β_z can range from 0 (i.e., no springs present) to infinity (i.e., fixed connection at L'). Examples of the effects of the modeled jamming fault condition on the first two auger tube frequencies for various values of L', κ_z, and β_z are provided in Fig. 13. The auger length and drill depth for this analysis are 1 and 0.5 m, respectively. The jam strength represents the intensity of the jamming condition where 0 reflects no jamming (i.e., κ_z and β_z are 0) and 1 reflects the most severe case of jamming (i.e., fixed condition at L'). The y axis (normalized frequency) is the jammed auger frequency normalized by the nominal drilling frequency.

This procedure has been repeated for each drilling fault using unique parameters (e.g., κ_z and β_z) to define and distinguish each model. Detailed descriptions of the formulation and evaluation of the drilling fault models are provided in Statham [32]. The developed models have been empirically validated via three field test campaigns, which are described in Sec. IV.

D. Automated Signal Analysis and Health Monitoring

The current application requires autonomous, real-time SHM that provides fault-diagnostic results on demand to the drill executive (the

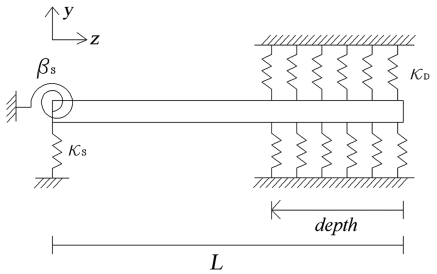

Fig. 10 Nominal drilling model.

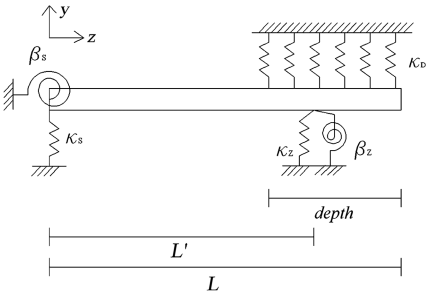

Fig. 12 Structural model of jamming drill fault.

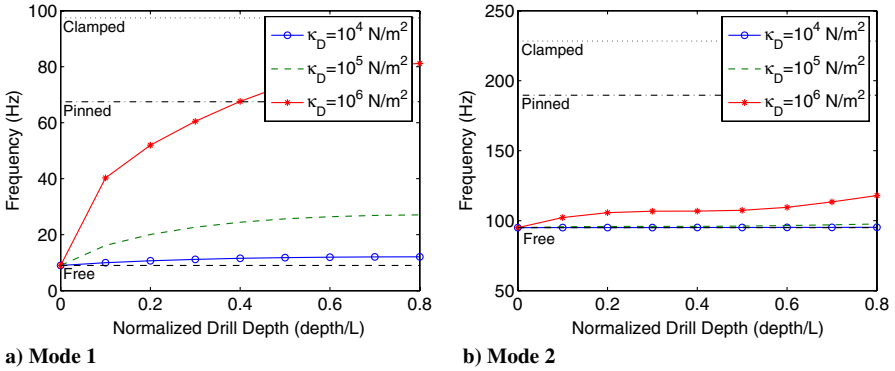

a) Mode 1 **b) Mode 2**

Fig. 11 Changes in natural frequency with drill depth (1-m auger).

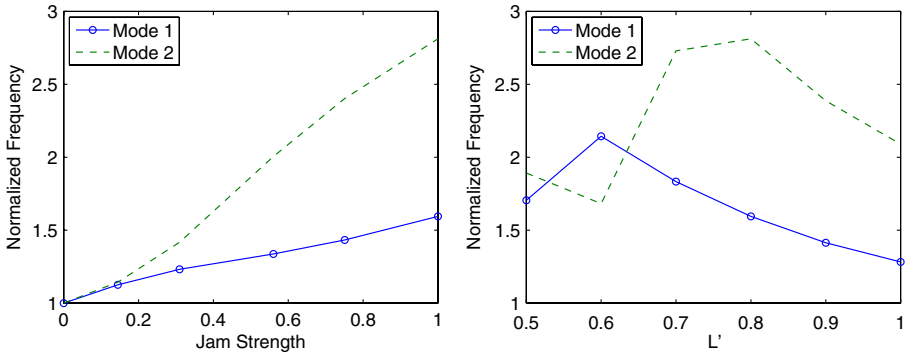

a) *L'* = 0.8 **b) Jam strength = 1**

Fig. 13 Effects of jamming condition on natural frequencies (1-m auger, 0.5-m depth).

computer/program that executes the drilling operation and interprets the fault-diagnostic results). Analyzing the dynamic response of the drill auger tube and providing real-time diagnostics is a challenging task for the formulation of the presented SHM technique. Most SHM techniques to date require time-intensive analysis of the dynamic response and are completed on representative structures or while the system is off-line (i.e., not in service) for maintenance. Conducting dynamic response experiments also involves many hands-on activities from initializing equipment to capturing data to analysis. Therefore, an automation procedure and the corresponding software are developed to control and operate these activities and network with the drill executive to relay all diagnostics, ensuring full autonomous operations of the SHM technique. Figure 14 shows a flowchart of the automation procedure, and details of the individual components are provided in the following subsections.

1. *Harmonic Frequency Filter*

It was determined, from the preliminary field tests and laboratory experiments, that the drill gearbox system produces harmonic frequencies in the dynamic response of the drill auger tube. (Note the incrementing peaks in Fig. 4.) These harmonic frequencies often dominate the signal and interfere with the signal analysis and diagnostics. Therefore, the development of a harmonic frequency filter to determine the location of the gear mesh frequencies in the signal response and filter them from the data set before the signal is analyzed further is necessary.

The equation used for determining the harmonic frequencies is based on a mathematical model formulated for the rotorcraft transmission vibration signal by McFadden [36] in 1987. Assuming a perfect gear system, the tooth meshing vibration is approximated by

$$\xi_{\text{perfect}}(t) = \sum_{n=0}^{\infty} \Xi_n \cos(\omega t + \Phi_n) + w(t) \tag{10}$$

where Ξ_n is the amplitude of the nth harmonic, ω is the mesh frequency given by $\omega = 2\pi f_r Q$, f_r is the gear rotation frequency, Q is the number of teeth, Φ_n is the phase angle of the nth harmonic, and $w(t)$ is noise often represented as Gaussian white noise [37]. According to this model, the harmonic components occur in increments related to the rotational frequency of the motor and the number of gear teeth. Thus, the following formula is used to determine the harmonic frequencies f_n:

$$f_n = Q f_r n, \qquad n = 1, 2, 3, \ldots \tag{11}$$

The drill system of interest uses a 90-gear tooth motor (i.e., $Q = 90$). Thus, the harmonic frequencies of the drill, rotating at 45 rpm or 0.75 Hz, occur at 67.5, 135, 202.5 Hz, etc. From experiments, Eq. (11) is an accurate model for predicting the harmonic motor gear frequencies.

To filter these harmonic frequencies from the signal response, a Chebyshev type I digital bandpass filter of order three is used. Chebyshev filters are infinite impulse response (IIR) filters and are commonly used in noise filtering processes [38,39]. The filter produces an nth order frequency domain function [40,41] in the form

$$H(z) = \frac{B(z)}{A(z)} = \frac{b_1 + b_2 z^{-1} + \ldots + b_{n+1} z^{-n}}{1 + a_2 z^{-1} + \ldots + a_{n+1} z^{-n}} \tag{12}$$

using the specified bandpass information, which can then be used to filter the signal response. Figure 15 provides the filtered response of the auger tube rotating in place at 45 rpm.

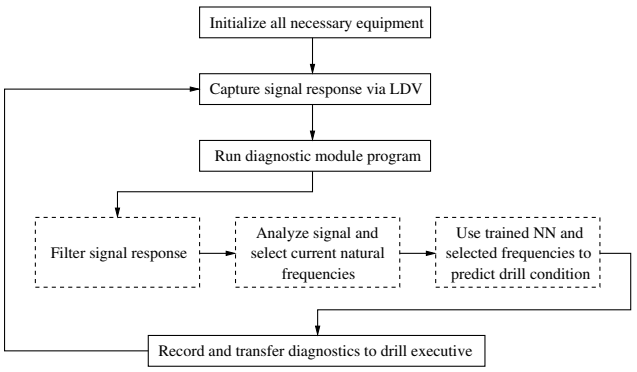

Fig. 14 Automation procedure for dynamics-based SHM.

2. *Automated Signal Analysis*

Once the dynamic signal of the drill auger tube is collected and filtered, analysis of the signal and identification of the natural frequencies are needed. To complete this process, an automated signal analysis algorithm has been developed. This algorithm defines a possible frequency range (based on the current drill depth and developed structural dynamic models) for the first two natural frequencies, and then selects the most probable peaks (maximum amplitudes) in the signal to quantify the current auger frequencies. The developed algorithm also takes into account that the harmonic frequency filter may unintentionally filter the auger frequencies if they are close to the gear mesh frequencies. Therefore, if two distinct auger frequencies are not found or if the magnitude of either peak is less than 30% of the maximum amplitude in the signal, it is assumed that the actual auger frequency was unintentionally filtered and the designated auger frequency is set equal to the nearest harmonic frequency. Examples of the harmonic frequency filter and the developed signal analysis algorithm applied to a simulated and actual drilling signal are provided in Fig. 16.

3. *Implementation of Neural Networks*

Inspired by biological nervous systems, artificial neural networks (NN) are composed of simple elements (neurons) operating in parallel, which are commonly adjusted, or trained, so that a particular input leads to a specific target output [42]. Neural networks have been trained to perform complex functions in various fields of

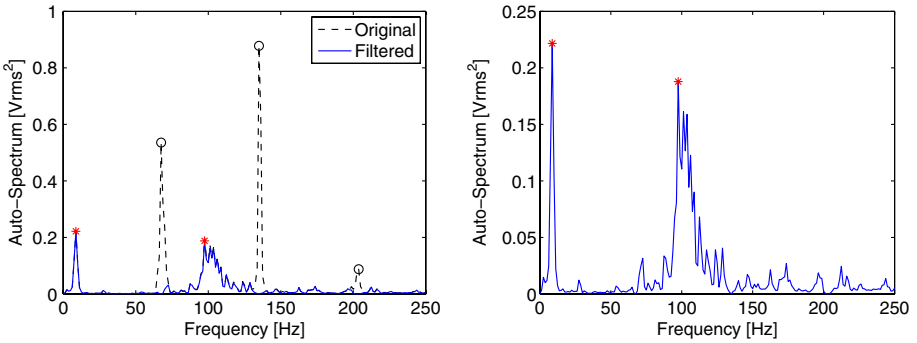

Fig. 15 Filtered rotating dynamic response of drill system at 45 rpm.

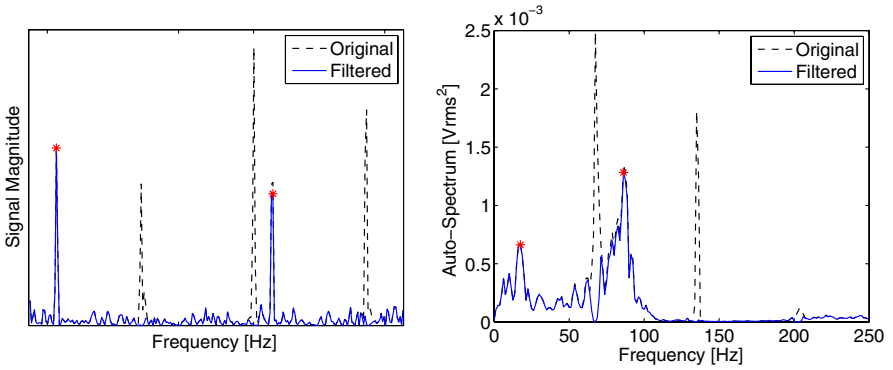

a) Simulated response with noise **b) Drilling auger tube signal**

Fig. 16 Signal analysis algorithm applied to dynamic response signals.

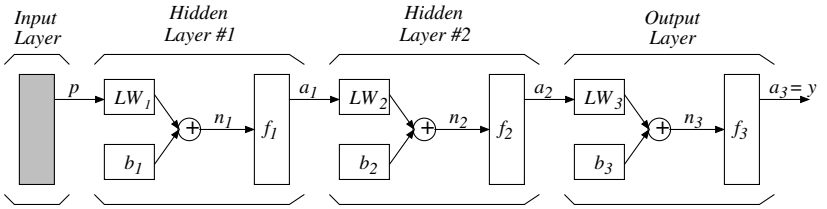

Fig. 17 Feed-forward multilayer neural network [42] (p = input values, LW_i = weights for layer i, b_i = biases, n_i = net input vector, f_i = transfer function, a_i = layer outputs, y = network output).

application, including pattern recognition, identification, control systems, and structural health monitoring [1,43–45].

The requirement for a rapid-response SHM system is addressed by the use of neural networks. Each structural dynamic model has a complicated characteristic equation and an infinite number of possibilities for each parameter (e.g., depth, jamming location, etc.). Using these characteristic equations directly to solve the model parameters and fault probabilities (similar to the procedure used to quantify the spring constants for the drill supports and nominal drilling model) is very cumbersome and time consuming, which are problematic when a rapid-response diagnostics system is required. This is resolved by creating an adequate database of various model parameters and their corresponding frequencies off-line and implementing a function approximation algorithm (such as neural networks [46]) that can be easily accessed online.

A feed-forward, backpropagation neural network is used in this research [42]. Feed-forward NNs allow signals to travel from input to output only and are extensively used in pattern recognition. A diagram of a feed-forward multilayer neural network is provided in Fig. 17. The backpropagation algorithm is a supervised, adaptive learning technique [47] that greatly improves the training process and accuracy of the NN results.

To train the neural networks, a database with various values for the model parameters (e.g., depth, jamming strength and location, etc.) and the corresponding natural frequencies is created for each drilling mode (nominal drilling and six drilling faults). Each individual neural network is then trained using the natural frequencies and drill depth as the input values and the probability of the drilling condition as the output. The probability of the drilling condition is based on the fault parameters for each drilling fault model. For example, the spring constants (κ_z and β_z) for the jamming fault model range from 0 to infinity, and the corresponding natural frequencies represent a 0 to 100% jamming fault probability. A diagram of the jamming fault NN is provided in Fig. 18.

This approach has been completed for all expected drilling conditions. Thus, for each signal response captured, the trained

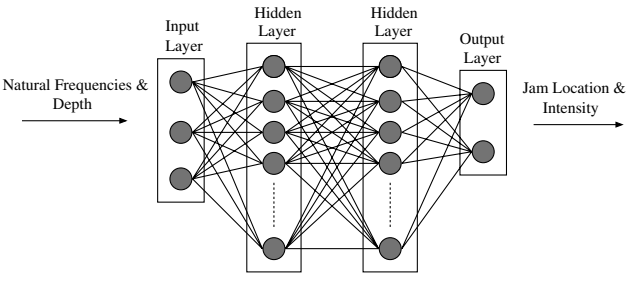

Fig. 18 Neural network structure of jam drilling fault.

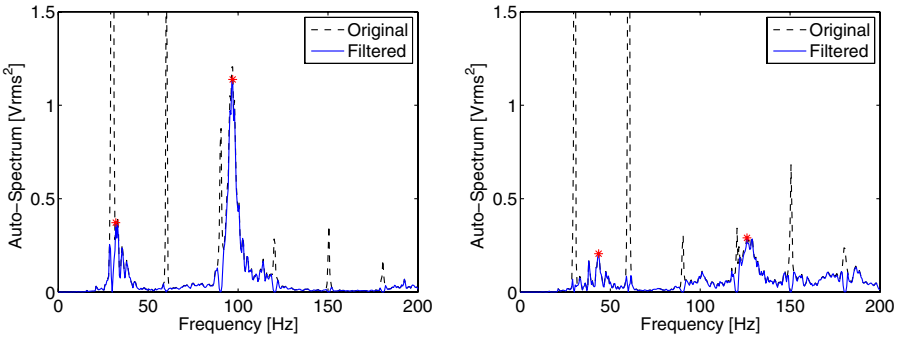

a) Before jamming fault **b) During jamming fault**

Fig. 19 Dynamic response of drill auger tube through a jamming fault.

neural networks are used to evaluate the probability of each drilling fault condition.

Lastly, although each structural dynamic model developed is unique, overlaps in the possible natural frequency values can occur. Therefore, to better isolate which drilling fault may be occurring and to reduce false positives, a heuristic filter based on the current drilling telemetry (auger torque, drill depth, down-hole force, etc.) has been developed. This filter uses the current drilling telemetry and quantified thresholds (based on design limits and field tests) to filter the neural network results and better identify the correct drilling fault. For example, if the neural network results show a similar probability for bit inclusion and binding, the auger torque and bit torque values are used to more accurately predict which fault mode is most probable.

4. Automation Procedure and Drill Interface

To complete the automation process for the diagnostic module program and network with the drill executive, a control program has been developed. This program, written in C++, interfaced the measurement equipment (LDV sensors and DAQ), diagnostic module program, and the drill executive (Fig. 14).

The DAQ equipment and associated software are first initialized, and the current auger tube signal is collected via the LDV sensors while the real-time drill telemetry values are collected from the drill executive. The diagnostic module program (which includes the frequency filter, signal analysis algorithm, and trained neural networks) is then executed and the diagnostic probabilities are output to the control program. Lastly, the diagnostic results are relayed to the drill executive. This process is repeated until the user terminates the executable.

The dynamics-based SHM system, comprising LDV sensors, structural dynamic models and trained neural networks, harmonic frequency filter, signal analysis algorithm, and automation procedure, has met all specified requirements. Field testing and validation of this system are presented in the following section.

IV. Field Testing and Validation

Three field tests have been conducted using the developed autonomous, real-time, dynamics-based SHM system with the DAME drill prototype. These three field tests are described with more detail in the following subsections.

A. Devon Island Field Test (2006)

A field test was conducted at HCRS on Devon Island in July 2006 [15]. The objectives of this field test were to operate hands off for at least 3 h, reach a drill depth of 3 m, and successfully encounter and recover from three drilling faults. The drill executive and diagnostic modules were fully integrated for this field test, which allowed complete autonomous drilling operations with fault-diagnostic and recovery capabilities.

The dynamics-based SHM system, which used two LDV sensors to capture the dynamic signal of the drill auger tube from the same position for redundancy, successfully detected the four drilling faults it was equipped to detect during this field test: binding, choking, jamming, and hard material. The original and filtered signal response of the drill auger tube during a jamming fault is provided in Fig. 19. The plots provided were just before (nominal diagnostics; 0% probability for all drilling faults) and at the jamming fault detection (60% probability). The determined natural frequencies are indicated with asterisks. A clear shift in the natural frequencies of the auger tube is evident from these plots, which was diagnosed as a jamming fault by the dynamics-based SHM system and validated by the drilling team's observations. For these measurements, the auger tube length was 3.75 m, the auger speed was 20 rpm, and the total drill depth was approximately 2.77 m.

In this field test, the dynamics-based SHM system and the DAME system as a whole met or exceeded all specified objectives. Automated drilling capabilities with reliable on-board diagnostic modules and recovery procedures were successfully demonstrated. The drill system also demonstrated detection and proper recovery from four drilling faults, 4.5 h of consecutive hands-off drilling and a total of 44 autonomous drilling hours, and the final drill depth was 3.22 m.

B. Jet Propulsion Laboratory Tests (2007)

In October 2007, tests and demonstrations at the Jet Propulsion Laboratory (JPL) in California were completed [48]. The objective of these tests and demonstrations was to complete hands-off, blind drilling tests to further show the drill system's robust and adaptive capabilities. It was also important to show repeatability of the drilling procedure and prognostic accuracy, which was difficult to accomplish during field tests on Devon Island given the unknown and unpredictable subsurface environment. The tests were considered "blind" as the contents and arrangements of the material test columns for drilling were unknown to the team.

Three independent LDV sensors were used to capture the signal response from three different directions for this demonstration. The LDV sensors were situated to collect the lateral vibrations from the front and side of the drill and the axial vibrations using a laser-quality mirror to offset the laser beam angle from the third LDV. This was the first field test for this setup and it proved to increase the accuracy and capabilities of the dynamics-based SHM system. The (unfiltered) signal response of the auger tube showing the transition from nominal drilling to a hard material fault (75% hard material probability) to a bit inclusion fault (100% bit inclusion probability) is provided in Fig. 20. Each signal response represented autospectrum in units of Volts RMS (root mean square) squared (Vrms^2). During this drilling test, the auger tube length was 2 m and the auger speed fluctuated from 20 to 25 rpm. The on-board sensors showed high auger and bit torque readings and low down-hole speed (rate of penetration). Based on the diagnostics and sensor data, it was hypothesized that the drill encountered a harder material, which triggered a hard material fault and successful recovery procedure. As the drill broke through the harder material, however, small chunks of the material remained at the bottom of the hole, causing a bit inclusion fault.

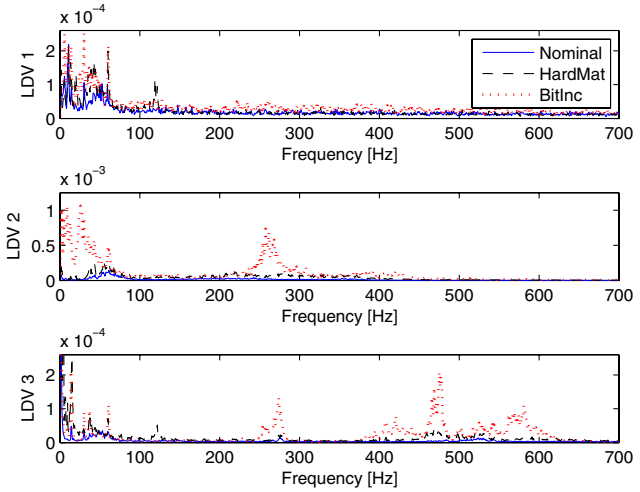

Fig. 20 Dynamic response (autospectrum in units of Vrms^2) of drill auger tube through nominal, hard material, and bit inclusion drilling conditions.

All specified goals and objectives were met during this test and demonstration at JPL. All three specimen columns were successfully drilled for a cumulative drilling depth of 2.96 m. The drill system demonstrated 35 total h of hands-off automated drilling, and five of the six drilling faults were detected and recovered from successfully. Choking, which is commonly associated with coarse or wet cuttings not progressing up the auger flutes to the surface, was not detected. These blind and reproducible tests were a rigorous mean to demonstrate and verify the fully integrated autonomous drill system's capabilities.

C. Devon Island (2008)

The third field test was at Devon Island in July 2008 [49]. The objectives of this field test were to integrate and test the upgraded drill executive, drill at a location with hydrothermal vents to a depth of 2 m, and collect subsurface samples at approximately every 25–50 cm for further geological analysis. Updates to the diagnostic modules based on the previous field tests and further laboratory tests were also implemented.

The three LDV sensor setup was again used for this field test. In addition to the neural network predictions based on the current drill signal, theoretical models, and heuristic filters, a boundary condition (BC)–based system was implemented to provide rapid-response diagnostics purely based on the current telemetry readings. To capture accurate measurements from the LDV sensors, the signal response is recorded and averaged, which produces diagnostics from the SHM system approximately every 20–25 s. As some drilling faults can occur instantaneously, in particular jamming, a parallel system was developed to analyze the drill telemetry for any sudden abnormal changes that breached or exceeded the drill system limitations. The BC-based system provided diagnostics to the drill executive every 2 s.

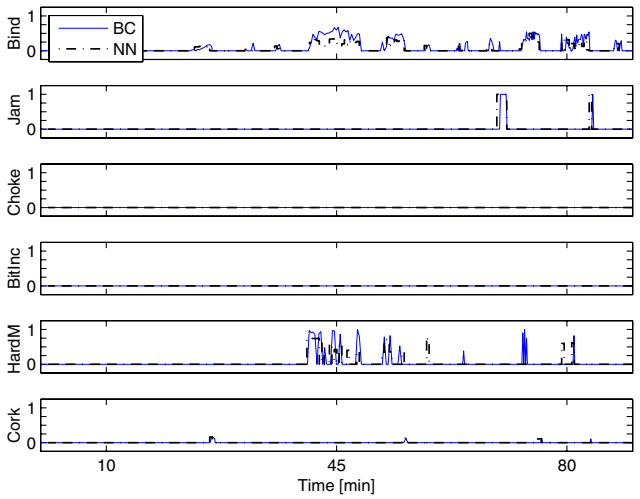

Fig. 21 Example of dynamics-based SHM system diagnostics.

An example of the results produced by the BC-based and signal-based systems over a test run in Devon Island are provided in Fig. 21. From this example, it is evident that the parallel systems were most often in agreement; however, there were some delays in the signal-based diagnostics to detect a fault (false negatives) or to detect that a potential fault was alleviated through nominal drilling operations (false positives). The BC-based system provided an additional heuristic filter for the dynamics-based diagnostics and a means for triggering fault conditions immediately if a drilling parameter breached an unsafe operating threshold.

During this field test campaign, the drilling team and the developed dynamics-based SHM system met or exceeded all specified objectives. A total of 32 h of autonomous, hands-off drilling was accomplished over five days, and a total drill depth of 2.02 m was achieved. Two diagnostic modules (rule-based and dynamics-based SHM) were used in parallel and demonstrated robust and reliable monitoring of the drilling operation, and five of the six drilling faults were detected and recovered successfully [49]. The BC-based system proved to be a reliable and beneficial addition to the dynamics-based SHM system, and the improved system was able to accurately predict all drilling fault conditions with even fewer false positives than previous field tests.

V. Conclusion

An autonomous, real-time, dynamics-based structural health monitoring system has been formulated for interplanetary drilling applications. As the requirements for an interplanetary exploration SHM system are beyond typical terrestrial requirements, new and innovative techniques were needed. These techniques included:

1) Using the drill motor system as an internal actuator for exciting the dynamic response of the drill.

2) Using noncontact laser Doppler velocimeter sensors to capture the dynamic response of the drill system.

3) Developing structural dynamic models for all expected drilling conditions (nominal and six drilling faults).

4) Developing a frequency filter to remove the rotating harmonic frequencies due to the gearbox system from the recorded signal.

5) Developing an automated signal analysis algorithm to identify the current natural frequencies of the drill auger tube.

6) Implementing trained neural networks to compare the current natural frequencies of the drill auger tube with the recorded frequencies from the structural dynamic models.

7) Developing an automation procedure and the corresponding software to create a complete autonomous dynamics-based SHM system.

The formulated SHM system has met all specified requirements for interplanetary exploration missions and has proven to be a valuable addition to the health monitoring procedure for the Drilling Automation for Mars Exploration prototype drill in three field tests. Many of the recommendations made by state-of-the-art reviews on SHM techniques have also been addressed and met in this research. The number and location of sensors has been limited due to the vast flexibility and capabilities of LDV technology and sensors. All modal analysis experiments have been conducted on the actual drill system, and the completed field campaigns have validated the SHM technique to accurately monitor the health of the drill system in its operating environment. The SHM technique is autonomous, eliminating human involvement and error in the analysis of the drilling condition. Lastly, as the produced diagnostics are probabilities of each drilling fault, this SHM technique provides diagnostic results to the drill executive to allow for preemptive action before a fault occurs or before a fault significantly affects the drilling operation.

Future research efforts include extending the SHM system to diagnose other possible fault conditions (such as bit failure) and material characterization, and developing more sophisticated techniques for multidimensional measurements and health monitoring. Further development is also needed for the LDV sensors (specifically, the current size, weight, and operating environment limitations) to ensure compatibility with interplanetary exploration missions.

Acknowledgments

Shannon Statham and Sathya Hanagud thank NASA for their continued support toward the research developed at Georgia Tech. These authors also thank Vinod Sharma, Massimo Ruzzene, Alla Balueva, Agnivesh Tomar, and Alessandro Spadoni for their contributions to the design and development of the dynamics-based SHM system, and Honeybee Robotics for their cooperation and assistance with the DAME drill.

References

[1] Sohn, H., Farrar, C., Hemez, F., Shunk, D., Stinemates, D., and Nadler, B., "A Review of Structural Health Monitoring Literature: 1996–2001," Los Alamos National Lab. TR LA-13976-MS, 2003.

[2] Doebling, S. W., Farrar, C. R., Prime, M. B., and Shevitz, D. W., "Damage Identification and Health Monitoring of Structural and Mechanical Systems from Changes in Their Vibration Characteristics: A Literature Review," Los Alamos National Lab. TR LA-13070-MS, 1996.

[3] Salawu, O. S., "Detection of Structural Damage Through Changes in Frequency: A Review," *Engineering Structures*, Vol. 19, No. 9, 1997, pp. 718–723. doi:10.1016/S0141-0296(96)00149-6

[4] Schwarz, B. J., and Richardson, M. H., "Experimental Modal Analysis," *CSI Reliability Week*, Vibrant Technology Inc., Orlando, FL, Oct. 1999, pp. 1–12.

[5] Li, X. Y., and Law, S. S., "Condition Assessment of Structures Under White Noise Excitation," *AIAA Journal*, Vol. 46, No. 6, 2008, pp. 1395–1404. doi:10.2514/1.30426

[6] Chiang, D.-Y., and Cheng, M.-S., "Modal Parameter Identification from Ambient Response," *AIAA Journal*, Vol. 37, No. 4, 1999, pp. 513–515. doi:10.2514/2.745

[7] Dimaragonas, A. D., "Vibration of Cracked Structures: A State of the Art Review," *Engineering Fracture Mechanics*, Vol. 55, No. 5, 1996, pp. 831–857. doi:10.1016/0013-7944(94)00175-8

[8] Cawley, P., and Adams, R. D., "The Location of Defects in Structures from Measurements of Natural Frequencies," *Journal of Strain Analysis for Engineering Design*, Vol. 14, No. 2, 1979, pp. 49–57. doi:10.1243/03093247V142049

[9] Adams, R. D., Cawley, P., Pye, C. J., and Stone, B. J., "A Vibration Technique for Non-Destructively Assessing the Integrity of Structures," *Journal of Mechanical Engineering Science*, Vol. 20, No. 2, 1978, pp. 93–100. doi:10.1243/JMES_JOUR_1978_020_016_02

[10] Gudmundson, P., "Eigenfrequency Changes of Structures Due to Cracks, Notches or Other Geometrical Changes," *Journal of the Mechanics and Physics of Solids*, Vol. 30, No. 5, 1982, pp. 339–353. doi:10.1016/0022-5096(82)90004-7

[11] Kim, J.-T., Ryu, Y.-S., Cho, H.-M., and Stubbs, N., "Damage Identification in Beam-Type Structures: Frequency-Based Method vs Mose-Shape-Based Method," *Engineering Structures*, Vol. 25, No. 1, 2003, pp. 57–67. doi:10.1016/S0141-0296(02)00118-9

[12] Farrar, C. R., and Doebling, S. W., "An Overview of Modal-Based Damage Identification Methods," *Proceedings of DAMAS Conference*, Sheffield, U.K., Los Alamos National Lab., Los Alamos, NM, June 1997.

[13] Doebling, S. W., Farrar, C. R., and Prime, M. B., "A Summary Review of Vibration-Based Damage Identification Methods," *Shock and Vibration Digest Journal*, Vol. 30, No. 2, 1998, pp. 91–105. doi:10.1.1.57.9721

[14] Blacic, J. D., Dreesen, D. S., and Mockler, T. T., "The 3rd Dimension of Planetary Exploration—Deep Subsurface Sampling," *AIAA Space 2000 Conference and Exposition*, AIAA 2000-5301, Reston, VA, Sept. 2000.

[15] Glass, B., Cannon, H., Hanagud, S., and Paulsen, G., "DAME: Planetary-Prototype Drilling Automation for Subsurface Access," *Astrobiology*, Vol. 8, No. 3, 2008, pp. 653–664. doi:10.1089/ast.2007.0148

[16] Paulsen, G., Mumm, E., Kennedy, T., Chu, P., Davis, K., Frader-Thompson, S., Petrich, K., and Glass, B., "Development of Autonomous Drills for Planetary Exploration," *37th Lunar and Planetary Science Conference*, Lunar and Planetary Inst., Houston, TX, 2006, p. 2358.

[17] Zacny, K., Bar-Cohen, Y., Brennan, M., Briggs, G., Cooper, G., Davis, K., Dolgin, B., Glaser, D., Glass, B., Gorevan, S., Guerrero, G., McKay, C., Paulsen, G., Stanley, S., and Stoker, C., "Drilling Systems for Extraterrestrial Subsurface Exploration," *Astrobiology*, Vol. 8, No. 3, June 2008, pp. 665–706. doi:10.1089/ast.2007.0179

[18] Bar-Cohen, Y., and Zacny, K., (eds.), *Drilling in Extreme Environments: Penetration and Sampling on Earth and other Planets*, Wiley, Hoboken, NJ, 2009, pp. 1–28, 347–546.

[19] Stoker, C. R., Lemke, L. G., Cannon, H., Glass, B., Dunagan, S., Zavaleta, J., Miller, D., and Gomez-Elvira, J., "Field Simulation of a Drilling Mission to Mars to search for Subsurface Life," *36th Lunar and Planetary Science Conference*, Lunar and Planetary Inst., Houston, TX, 2005, p. 1537.

[20] Stoker, C. R., Lemke, L. G., Cannon, H., Glass, B., Dunagan, S., Zavaleta, J., Miller, D., and Gomez-Elvira, J., "The Search for Subsurface Life on Mars: Results from the MARTE Analog Drilling Experiment in Rio Tinto, Spain," *37th Lunar and Planetary Science Conference*, Lunar and Planetary Inst., Houston, TX, 2006, p. 1537.

[21] Glaser, D., Paulsen, G., Zacny, K., Davis, K., Mumm, E., and Glass, B., "Autonomous Drills for Planetary Subsurface Access," *LPI Space Resources Roundtable VIII*, Lunar and Planetary Inst., Houston, TX, Nov. 2006, p. 1020.

[22] Statham, S., Hanagud, S., Ruzzene, M., Glass, B., and Cannon, H., "Design and Validation of an LDV-Based Structural Health Monitoring in 'Drilling Automation for Mars Exploration'," *48th AIAA SSDM Conference*, AIAA, April 2007.

[23] Carden, E. P., and Fanning, P., "Vibration Based Condition Monitoring: A Review," *Structural Health Monitoring*, Vol. 3, No. 4, 2004, pp. 355–377. doi:10.1177/1475921704047500

[24] Lee, P., Bunch, T. E., Cabrol, N., Cockell, C. S., Grieve, R. A. F., McKay, C. P., Jr., Rice, J. W., Schutt, J. W., and Zent, A. P., "Haughton-Mars 97—I: Overview of Observations at the Haughton Impact Crater, A Unique Mars Analog Site in the Canadian High Arctic," *24th Lunar and Planetary Science Conference*, Lunar and Planetary Inst., Houston, TX, 1998, p. 1973.

[25] Lee, P., and Osinksi, G. R., "The Haughton-Mars Project: Overview of Science Investigations at the Haughton Impact Structure and Surrounding Terrains, and Relevance to Planetary Studies," *Meteoritics & Planetary Science*, Vol. 40, No. 12, 2005, pp. 1755–1758. doi:10.1111/j.1945-5100.2005.tb00144.x

[26] Zacny, K. A., and Cooper, G. A., "Methods for Cuttings Removal from Holes Drilled on Mars," *Mars*, Vol. 3, Dec. 2007, pp. 42–56. doi:10.1555/mars.2007.0004

[27] DSP Technology Inc., *SIGLAB User Guide: S2022D1/A*, San Jose, CA, 2001.

[28] Drain, L., *The Laser Doppler Technique*, Wiley, New York, 1980.

[29] Castellini, P., Martarelli, M., and Tomasini, E., "Laser Doppler Vibrometery: Development of Advanced Solutions Answering to Technology's Needs," *Mechanical Systems and Signal Processing*, Vol. 20, No. 6, 2006, pp. 1265–1285. doi:10.1016/j.ymssp.2005.11.015

[30] Sharma, V. K., Hanagud, S., and Ruzzene, M., "Damage Index Estimation in Beams and Plates Using Laser Vibrometry," *AIAA Journal*, Vol. 44, No. 4, April 2006, pp. 919–923. doi:10.2514/1.19012

[31] Statham, S., Hanagud, S., Sharma, V., and Glass, B., "Three-Dimensional Structural Health Monitoring in Space Applications Using Laser Doppler Vibrometers," *49th AIAA SSDM Conference*, AIAA, April 2008.

[32] Statham, S. M., *Autonomous Structural Health Monitoring Technique for Interplanetary Drilling Applications Using Laser Doppler Velocimeters*, Ph.D. Thesis, Georgia Inst. of Technology, Atlanta, GA, 2011.

[33] Tekinalp, O., and Ulsoy, A. G., "Modeling and Finite Element Analysis of Drill Bit Vibrations," *Journal of Vibration, Acoustics, Stress, and Reliability in Design*, Vol. 111, No. 2, 1989, pp. 148–155. doi:10.1115/1.3269835

[34] Rincon, D. M., and Ulsoy, A. G., "Complex Geometry, Rotary Inertia

and Gyroscopic Moment Effects on Drill Vibrations," *Journal of Sound and Vibrations*, Vol. 188, No. 5, 1995, pp. 701–715. doi:10.1006/jsvi.1995.0619

[35] Huang, B. W., "Dynamic Characteristics of a Drill in the Drilling Process," *Proceedings of the Institution of Mechanical Engineers, Part B: Journal of Engineering Manufacture*, Vol. 217, No. 2, 2003, pp. 161–167. doi:10.1243/095440503321148803

[36] McFadden, P., "Examination of a Technique for the Early Detection of Failure in Gears by Signal Processing of the Time Domain Average of the Meshing Vibration," *Mechanical Systems and Signal Processing*, Vol. 1, No. 2, 1987, pp. 173–183. doi:10.1016/0888-3270(87)90069-0

[37] Samuel, P. D., and Pines, D. J., "A Review of Vibration-Based Techniques for Helicopter Transmission Diagnostics," *Journal of Sound and Vibration*, Vol. 282, Nos. 1–2, 2005, pp. 475–508. doi:10.1016/j.jsv.2004.02.058

[38] Pahk, H. J., Lee, D. S., and Park, J. H., "Ultra Precision Positioning System for Servo Motor-Piezo Actuator Using the Dual Servo Loop and Digital Filter Implementation," *International Journal of Machine Tools & Manufacture*, Vol. 41, No. 1, 2001, pp. 51–63. doi:10.1016/S0890-6955(00)00061-4

[39] Losada, R. A., *Digital Filters with MATLAB*, TR, The MathWorks, Inc., Natick, MA, May 2008.

[40] The MathWorks, Inc., *Signal Processing Toolbox User's Guide 6.13*, Natick, MA.

[41] Brown, R. G., and Hwang, P. Y. C., *Introduction to Random Signals and Applied Kalman Filtering: With MATLAB Exercises and Solutions*, Wiley, New York, 1997.

[42] Demuth, H., and Beale, M., *Neural Network Toolbox User's Guide*, The MathWorks, Inc., Natick, MA, 1992, pp. 1-4–1-15, 2-2–2-30.

[43] Luo, H., and Hanagud, S., "Dynamic Learning Rate Neural Network Training and Composite Structural Damage Detection," *AIAA Journal*, Vol. 35, No. 9, 1997, pp. 1522–1527. doi:10.2514/2.7480

[44] Pidaparti, R. M., Jayanti, S., Palakal, M. J., and Mukhopadhyay, S., "Structural Integrity Redesign Through Neural-Network Inverse Mapping," *AIAA Journal*, Vol. 41, No. 1, 2003, pp. 119–124. doi:10.2514/2.1920

[45] Yang, S. M., and Lee, G. S., "Structural Damage Identification Using Pole/Zero Dynamics in Neural Networks," *AIAA Journal*, Vol. 39, No. 9, 2001, pp. 1805–1808. doi:10.2514/2.1515

[46] Annema, A.-J., *Feed-Forward Neural Networks: Vector Decomposition Analysis, Modelling and Analog Implementation*, Kluwer Academic Publishers, Norwell, MA, 1995, pp. 1–19.

[47] Widrow, B., and Lehr, M. A., "30 Years of Adaptive Neural Networks: Perceptron, Madaline, and Backpropagation," *Proceedings of IEEE*, Vol. 78, No. 9, Sept. 1990, pp. 1415–1442. doi:10.1109/5.58323

[48] Glass, B., Christa, S., Hanagud, S., Statham, S., Mukherjee, S., Shirashi, L., Paulsen, G., and Cohen, J., "Planetary Drilling Automation Blind Tests," *39th Lunar and Planetary Science Conference*, Lunar and Planetary Inst., Houston, TX, March 2008, p. 2126.

[49] Glass, B., Thompson, S., Hanagud, S., Statham, S., Cohen, J., Lee, P., Osinksi, G., and Huffman, S., "Planetary Drill Prototype Testing at an Impact Structure Palaeo-Hydrothermal Site," *40th Lunar and Planetary Science Conference*, Lunar and Planetary Inst., Houston, TX, 2009, p. 2197.

B. Epureanu
Associate Editor